Available online at www.sciencedirect.com
ScienceDirect
Nuclear Instruments and Methods in Physics Research A 566 (2006) 338–350
NUCLEAR INSTRUMENTS & METHODS IN PHYSICS RESEARCH Section A
www.elsevier.com/locate/nima

Production technique and quality evaluation of CsI photocathodes for the ALICE/HMPID detector

H. Hoedlmoser[a,*], A. Braem[a], G. De Cataldo[a,b], M. Davenport[a], A. Di Mauro[a], A. Franco[b], A. Gallas[b], P. Martinengo[a], E. Nappi[b], F. Piuz[a], V. Peskov[a], E. Schyns[a]

[a]*CERN, Switzerland*
[b]*INFN-Sez. di Bari, Bari, Italy*

Received 15 June 2006; accepted 18 July 2006
Available online 14 August 2006

Abstract

The ALICE/HMPID detector has been equipped with 42 large area CsI photocathodes providing a total of 11 m^2 of photosensitive area for the detection of Cherenkov light. This production summary reports on the CsI coating procedure and provides results of the quality monitoring measurements by means of a photocurrent scanner system. The importance of the heat enhancement of CsI PCs is stressed and difficulties due to variations in this process are presented, followed by a discussion of possible influences of production parameters on this process.

PACS: 25.6; 34.8a

Keywords: CsI photocathode; Heat enhancement; RICH; HMPID

1. Introduction

The ALICE High Momentum Particle Identification (HMPID) detector [1,2] consists of seven RICH detector modules covering a total sensitive area of 11 m^2. It features a proximity focussing layout in which the primary ionizing particle generates Cherenkov light inside a liquid C_6F_{14} radiator. The UV photons are converted into photo-electrons inside the 300 nm thin CsI film of the photo-cathodes (PCs) and the photo-electrons are amplified in an avalanche process inside a Multi-Wire Proportional Chamber (MWPC). The detector signal is read out from the PC which is segmented into pads (8 mm × 8.4 mm) to allow the reconstruction of the Cherenkov rings. Details about the technical design are given in Ref. [2] and the current status of the ALICE HMPID project is described in Ref. [6]. The content of this paper focuses on the production of the 42 CsI PCs necessary to equip the seven detector modules in a dedicated CsI coating facility at CERN, describing in detail the production procedure from substrate preparation and coating process to the quality monitoring (Section 2) carried out by means of a VUV-scanner system which is integrated into the production setup—see Fig. 1 and Refs. [3,8,9]. A summary of the results of the production is presented providing information on relative and absolute QE of the PCs and on quality variation across the PC surface and from PC to PC. The importance of post deposition heat enhancement to meet detector requirements and its responsibility for the mentioned quality variations are stressed. Several of the production parameters have been investigated regarding their influence on the enhancement process, e.g. it was confirmed that the substrate quality is not directly determining the effectiveness of the enhancement.

2. Procedure for PC production and quality monitoring

Details about the PCs and the production procedures have been published in Refs. [4,5]. With the availability of the VUV-scanner [3,8,9] providing immediate feedback on

*Corresponding author.
E-mail address: herbert.hoedlmoser@cern.ch (H. Hoedlmoser).

0168-9002/$ - see front matter © 2006 Elsevier B.V. All rights reserved.
doi:10.1016/j.nima.2006.07.047

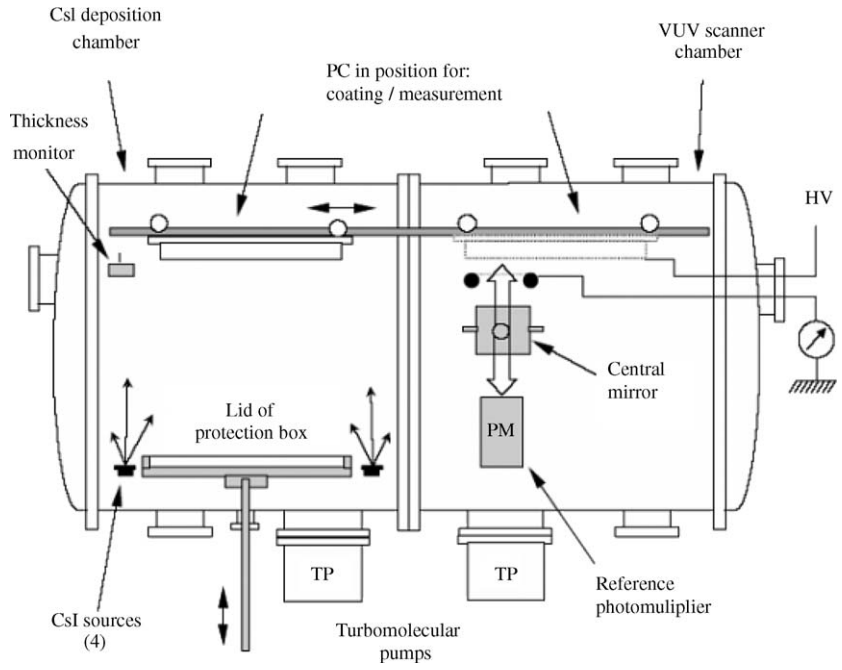

Fig. 1. Layout of the CsI production chamber. Left: CsI evaporation side, right: photo-current measurement side. The reader is referred to Refs. [2,3,8,9] for detailed descriptions of the plant.

the effectiveness of the production procedures, the process could be fine tuned to obtain the best results and overcome some problems mentioned in Sections 3.1 and 4. Therefore the following paragraph repeats the basic steps of the production procedure emphasizing recent changes. Furthermore, the quality monitoring procedures subsequent to coating are described.

The substrate for the CsI PCs described in Refs. [4,5] is a double layer Cu clad PCB coated with Ni and Au segmented into pads for the position sensitive readout. After being glued onto an aluminium frame the substrates undergo an elaborate sequence of cleaning and testing procedures (cleaning with strong detergents, ultrasonic baths, demineralized water, pure alcohol, tests of gas-tightness and high-voltage capability within the MWPC). Subsequently the substrates arrive at the CsI deposition facility, where they are cleaned again with demineralized water, alcohol and nitrogen jet, followed by one day in a drying oven at 60 °C before they are finally installed in the CsI evaporation plant. Detailed descriptions of the plant can be found in Refs. [2,9] and the basic layout is given in Fig. 1. After the installation of the substrate in the 1000 l vacuum chamber the system is pumped for a minimum of two days. With the start of the pumping cycle the temperature of the chamber is increased to 60 °C within a few hours by means of a heating tape enclosing the whole vessel. The final pressure achieved in the chamber before CsI deposition is approximately 6×10^{-7} mbar with a composition of 80–90% water and 3–10% hydrocarbons—Fig. 2 shows a typical residual gas composition, which is routinely measured prior to CsI deposition.

Recently even longer pumping cycles up to three days have been favoured to allow more time for the slow process of water removal from the chamber walls. During installation (and extraction procedures) the chamber is kept open to air for the minimum time necessary and it is being kept at a temperature higher than the environment (typically 30 °C) at all stages to minimize adsorption of humidity in the hygroscopic CsI layers present in the chamber from previous evaporations. Only when it fits into the production schedule, the chamber is cleaned to avoid accumulating too much CsI on the walls; however, good results have been obtained after up to 15 evaporation cycles without cleaning. The CsI deposition is carried out with the full system at 60 °C. The evaporation is performed by means of resistive heating of four molybdenum boats each filled with 0.75 g pre-melted CsI powder and symmetrically arranged below the substrate. The heating current running through the sources is increased slowly (within 15–30 min) until the evaporation starts. Recently the process was slowed down further to $\geqslant$30 min as some of the PCs with faster ramp up times ($\approx$ 15 min) showed problems. During the evaporation the deposition rate is kept at $\approx$ 1 nm/s with the help of two quartz thickness monitors and labview software. Given the precise amount of pre-melted source material a final layer thickness of 300–325 nm is achieved.[1] After CsI deposition, the PC is immediately transferred to the VUV-scanner which is integrated into the chamber (Fig. 1) and allows an in situ scan of the photo-current across the whole PC surface. The system was described in

[1]Both the calculation of the thickness from the amount of evaporated CsI and the measurement using the thickness monitors relies on the assumption of a density similar to the bulk material for the deposited coating—see discussion in Section 5.

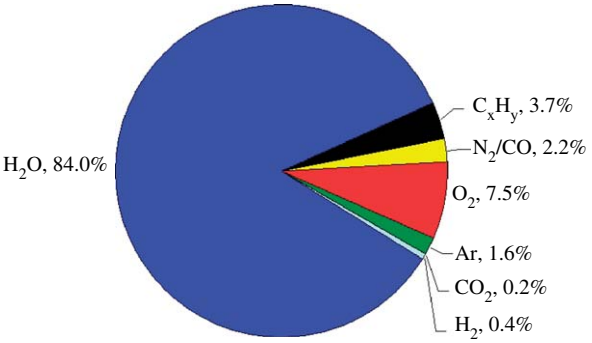

Fig. 2. Typical composition of the residual gas measured prior to CsI evaporation.

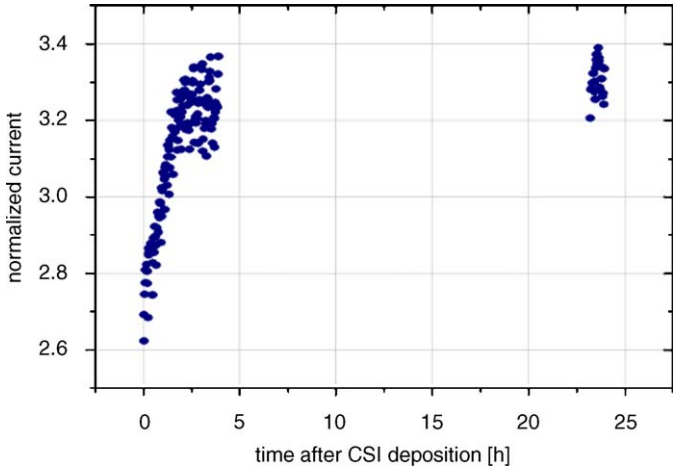

Fig. 3. Development of $\langle I_{\text{norm}} \rangle$ during heat enhancement phase for several positions on PC57v2 after a deposition on a hot substrate (both PC and deposition plant at $T = 60\,^{\circ}\text{C}$).

Refs. [3,9]. The PC response is monitored during the heat-conditioning phase as described in Section 3.1. Afterwards the system is cooled down to room temperature to perform the final mapping of the photo-current before the extraction of the PC from the plant. In preparation for the extraction procedure the chamber is filled with dry Ar gas and the PC is enclosed in a protective box at atmospheric Ar pressure to avoid any contact of the highly hygroscopic CsI layer with humid air, which is known to destroy the PC. The enclosed PC is then extracted from the deposition plant and connected to Ar flow until transfer to the detector modules.

3. Quality monitoring of CsI PCs

The PC quality is measured by means of the VUV-scanner which performs a 2D mapping of the photo-current from the CsI PC resulting from an illumination with a beam of UV light [3,9]. The photo-current I_{CsI} from the PC is recorded as well as the reference signal I_{PM} from a CsI photomultiplier (PM) (read from the first dynode) and the background levels I_{CsInoise} and I_{PMnoise}. The reference current on the PM is used to normalize the photo-current from the PC according to $I_{\text{norm}} = (I_{\text{CsI}} - I_{\text{CsInoise}})/(I_{\text{PM}} - I_{\text{PMnoise}})$. The currents are measured without amplification in the range of approximately 50–500 pA, whereas the background currents are <1 pA. I_{norm} has a typical value between 3 and 3.8. A repeated measurement on a single spot on a PC including repositioning of the spot shows a reproducibility of 98%.

3.1. Heat enhancement of the photo-current

The quality of a CsI PC is known [2,10,11,14] to depend on the treatment after coating. Initially the QE is rather low but it increases—especially in the low wavelength range ($\geqslant$190 nm) if the PC is heated to 60 °C for several hours after deposition or if the deposition is already performed on a hot substrate. With the completion of the VUV-scanner it was possible for the first time to measure these enhancement effects on the large area PCs produced at CERN by monitoring the photo-current from several positions on a PC in time during the enhancement phase [3]. Multiple tests have been performed with both evaporations at 60 °C and evaporations at room temperature with subsequent heating [9]. Fig. 3 shows the development of the normalized current in time as measured during the enhancement phase on several positions on a PC, which was produced according to the standard procedure described above. The deposition was performed at 60 °C and the PC was kept at this temperature for more than a day after CsI deposition. The spread of the data points on the current axis reflects the spatial inhomogeneity of the PC efficiency across the PC surface—see Section 3.2. Normally the photo-current increases by 20–50% within the first 2–10 h after coating.[2] Both the rate of increase and the achieved final level of the normalized current show a considerable variation.

The plot in Fig. 4 shows the average current level for each produced PC. The grey symbols show the current levels before enhancement measured within 20 min after the CsI deposition at high temperature (60 °C). The black symbols show the final level after the enhancement phase is completed, and the PC is cooled down to room temperature before the PC is extracted from the plant. From the comparison it follows that the quality spread from PC to PC is rather small before the enhancement starts, whereas the PC quality shows a spread of up to 33% after enhancement. Approximately 20% of all produced PCs (including test evaporations) exhibited a total lack or interruption of the initial enhancement effect, thus providing the main contribution to the large spread. This problem will be discussed in detail in Section 4. In some cases these

[2]Due to wavelength dependence of the enhancement effect mentioned above, the increase depends on the source spectrum used in the measurement and can change if different windows or filters are used in the optics.

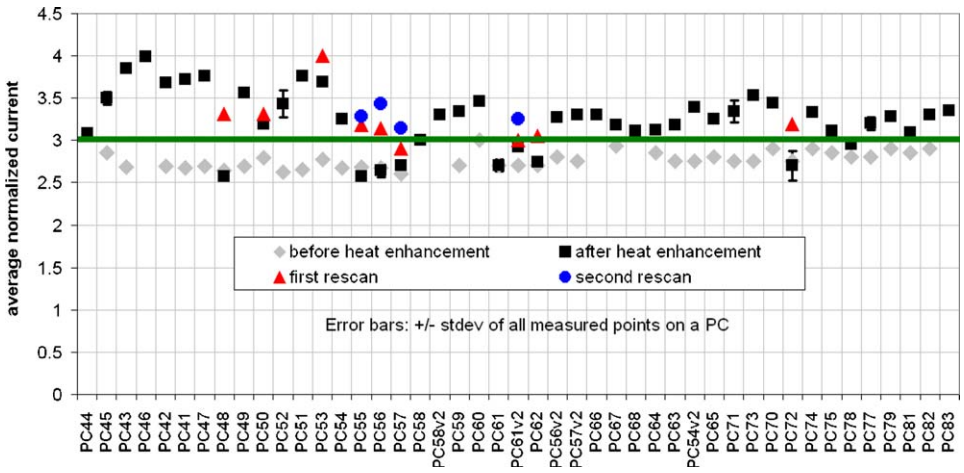

Fig. 4. Comparison of the average level of normalized current of all produced PCs before heat enhancement, before extraction from the plants and from later rescans weeks/months after production. The green line defines the minimum requirement to accept the PC for use on the detector [3].

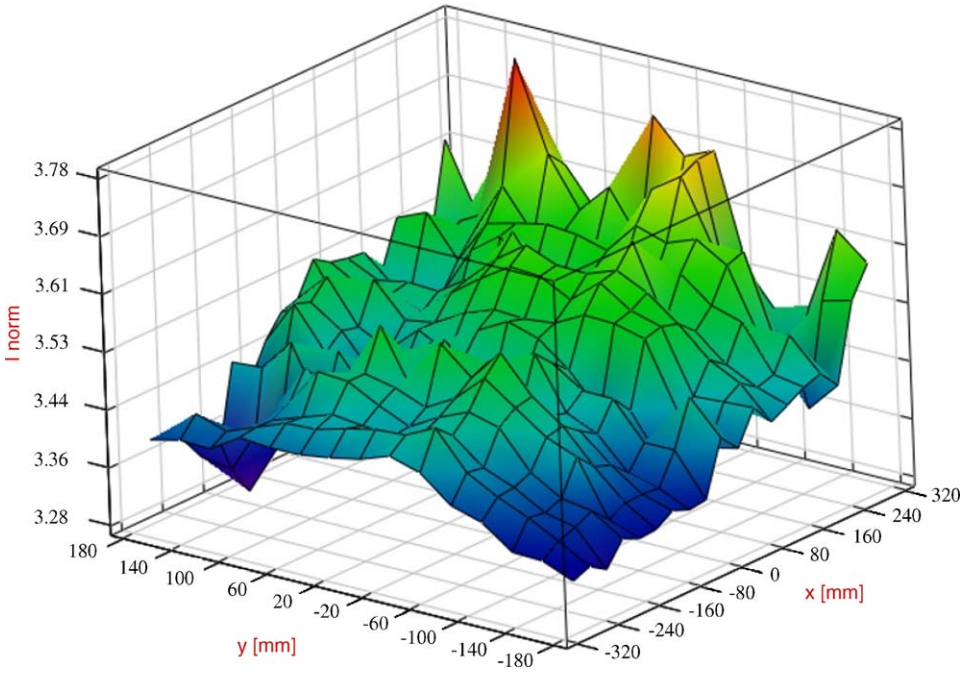

Fig. 5. Mapping of I_{norm} across the surface of PC 45. The 6% min–max spread of the quality is emphasized by the zero suppressed current axis.

PCs could be successfully recoated or they showed a much slower enhancement over several weeks or even months in storage under Ar gas-flow and all the PCs could finally be recuperated for use on the detector. This behaviour is reflected in the results of the re-scans in Fig. 4, which were conducted weeks or in some cases even months after production following beam tests or additional treatments as will be described in Section 4.3. The re-scans involved transferring the PCs from the detector or from storage back to the VUV-scanner, where they were opened under pure Ar before pumping down the system for the measurements, which were carried out at room temperature.

3.2. Comparative measurements and acceptance criteria

After the enhancement phase is completed and the PC is cooled down to room temperature, a scan covering 280 points equally spread over the PC is performed. Usually 6–12% minimum to maximum variation of the normalized current across the PC surface can be measured. Fig. 5 shows an example of such a surface mapping. Section 4.6 in Ref. [9] is dedicated to show that the measured variations are not caused by any systematic effects related to the scanner.

The average normalized currents $\langle I_{\mathrm{norm}} \rangle$ of the 280-point mappings are used to compare the PC quality, as in Fig. 4.

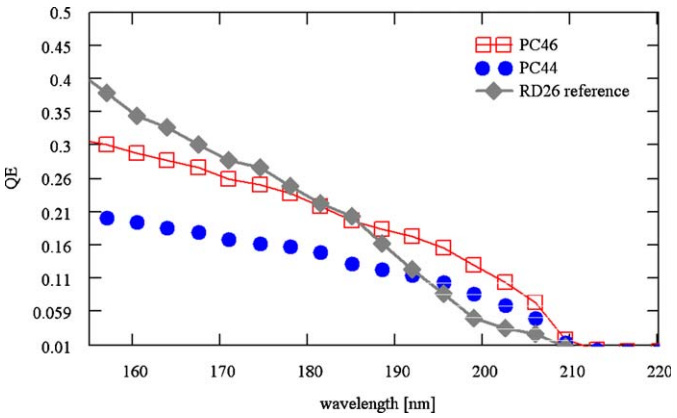

Fig. 6. Example of absolute QE for two PCs derived from a Monte Carlo analysis of test beam results in comparison to the reference QE obtained by the CERN-RD26 project for small samples.

The lower level for acceptance of $\langle I_{\text{norm}} \rangle = 3$ which is also shown in Fig. 4 was derived from a comparison of the scans of the first 17 PCs with test beam results[3] as described in Ref. [3]. PCs with $\langle I_{\text{norm}} \rangle = 3$ provide a minimum of 16 resolved clusters per Cherenkov ring in the beam tests which is sufficient to achieve the required detector performance.

3.3. Production summary and QE

Fig. 4 shows the quality level of all PCs which were mounted on the detector.[4] The final level of the average current $\langle I_{\text{norm}} \rangle$ of the accepted PCs shows a minimum to maximum variation from 3.05 to 4 with a mean value of 3.42. From the analysis of test beam results of several PCs absolute QE can be derived by Monte Carlo simulation [7]. Fig. 6 shows an example of QE plots for two of the PCs in comparison with the reference QE obtained by the CERN-RD26 project for small samples.

4. Investigation of quality variations

The lack of enhancement exhibited by some of the PCs poses a problem for several reasons. First of all the non-enhanced PCs do not immediately meet the minimum requirement imposed by the necessary detector performance and even though the PCs have shown a long time enhancement, which makes them eventually reach the requirements, there is the problem of the final characterization of the PC quality in order to provide QE data for the physics analysis once the detector is running. Due to time constraints, the quality mapping has to be performed after the production before the PCs are extracted from the coating facility. To re-scan all PCs at a later stage takes too much time and involves also quite some risk of exposure: the system was designed to safely enclose and extract a CsI PC under Ar atmosphere, but the reverse process mentioned above is much more elaborate. Consequently, the problem has been addressed in several lines of investigations. As described in Sections 4.1 and 4.2 an attempt was made to find correlations between production conditions (substrate quality, vacuum quality, evaporation rates, etc.) and the striking difference in the behaviour of PCs during the enhancement as visible in the comparison of the two time evolution types shown in Fig. 7. In the unsuccessful type (b) the enhancement of the photo-current is interrupted by a short decrease followed by a much slower enhancement which can last up to several months. For the two different types of time evolution in Fig. 7, the terms "successful enhancement" for case (a) and "unsuccessful enhancement" for case (b) were adopted, although "unsuccessful" is only correct from the point of view of the series production, which suffers a delay. It will be shown in Section 4.3 that even the type (b) PCs could be recuperated for use on the detector by means of additional treatments. However, to avoid any confusion, the type (b) PCs will be always referred to as "unsuccessfully enhancing" or "badly performing" PCs in the following text.

4.1. Exclusion of any direct influence of the substrate

A number of tests, including CsI depositions on samples of different substrates and re-coating of old substrates, were performed to exclude a responsibility of the substrate quality for the unsuccessful enhancement of some PCs. In addition to some previous results [3], which show that in a simultaneous coating of different substrate types most of the samples behave the same way, the following tests were performed:

(1) Inclusion of Au-coated glass substrates as witness samples in CsI depositions on standard PCB substrates.
(2) Coating procedures with the absence of any PCB from the chamber.
(3) Successful re-coating of badly performing PCs.

In the first step Au-coated glass substrates ($5 \times 5\,\text{cm}^2$ glass substrates coated with 10 nm Cr and 100 nm Au) were included in the CsI deposition procedure of the standard PCs as a reference. In all the CsI depositions performed since the introduction of this procedure, it was found that the behaviour and development of the samples follow the one of the standard PCs. Fig. 7 shows two results, one with the successful enhancement behaviour, in which the PC response increases and stabilizes, and the other one with the unsuccessful behaviour, in which the enhancement is interrupted by a decrease in performance. In both cases the samples exhibit the same behaviour as the large area PC. As the witness samples are completely different from the standard PCB substrates from the point of view of outgassing properties, cleaning procedure and surface roughness, these results indicate that the varying behaviour

[3]Test beam measurements were only available until November 2004.
[4]The plot includes PCs which were recoated and which were used for ageing tests.

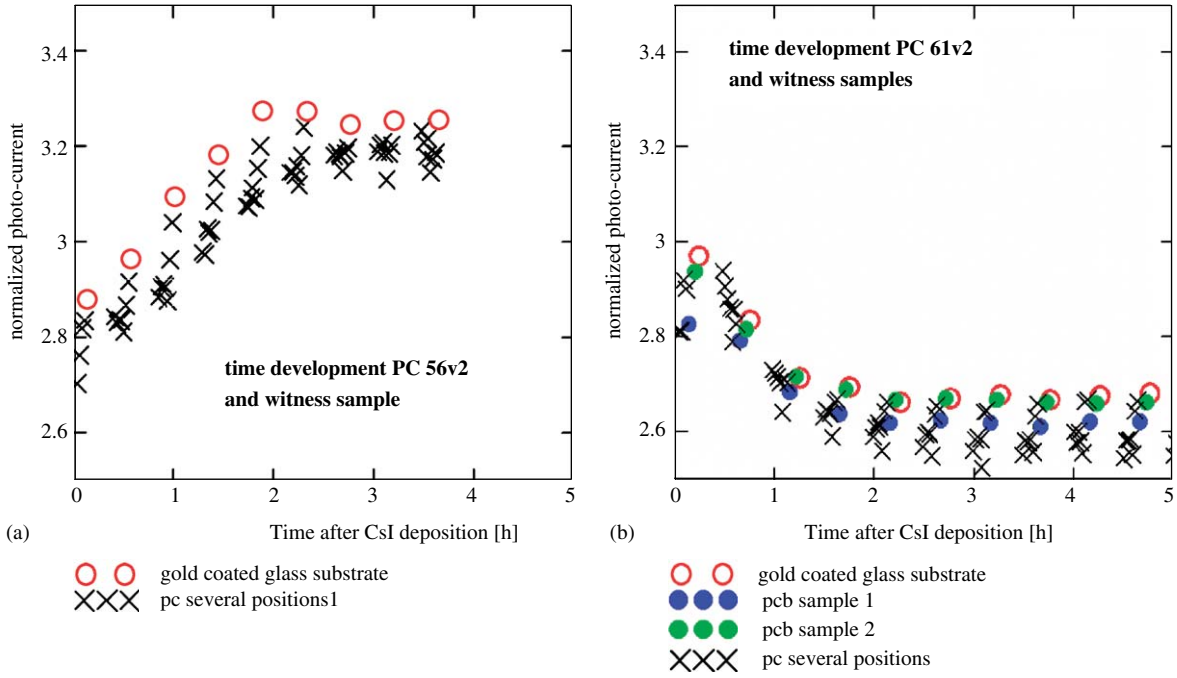

Fig. 7. (a) Successful and (b) unsuccessful heat enhancement following two CsI depositions carried out at 60 °C on standard substrates and witness samples.

of the PCs in the post treatment is not directly related to the nature of the substrate, unless the presence of the large area PCB substrate contaminates the whole chamber and leads to a change in the process.

In the next step test evaporations were performed only on Au–Cr-coated glass substrates with no PCB present in the vacuum chamber. In two test evaporations (T11 and T12) both the successful heat enhancement and the unsuccessful interrupted increase could be reproduced on these samples. A comparison of the enhancement phase in these two tests is given in Fig. 8. The result shows that the bad behaviour is not caused by the presence of the PCB material, e.g. by strong outgassing. The fact that the evaporation chamber was thoroughly cleaned in between the two tests indicates that the reason for the varying behaviour is linked to the status of the chamber itself and particularly to the presence of CsI layers in the chamber which are potentially filled with water—see discussion in Section 5.

Several of the PCs exhibiting an interrupted QE increase or no increase at all in the heat treatment phase have been cleaned by removing the CsI layer with demineralized water and subsequently recoated. PCs 54 and 56–58 showed good results after the second coating process and PC 61 showed a very slow enhancement afterwards. Some of these PCs—e.g. 56 and 57—had already shown a long term improvement after storage or additional treatments (see Section 4.3 before the re-coating.

The results of these tests combined with the previous results of studies with different substrates [3] indicate that there is no direct influence of the substrates used in our tests.

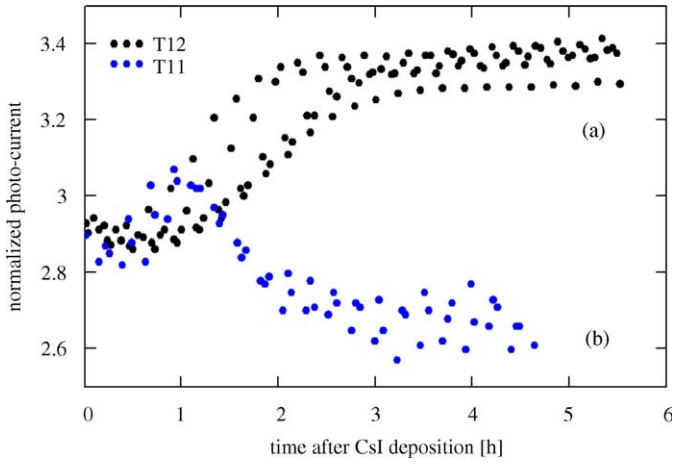

Fig. 8. Reproduction of two types of enhancement behaviour on Au-coated glass samples with no PCB substrate present in the chamber.

4.2. Correlations with coating process parameters

In the search for the cause of the varying enhancement behaviour a large number of production parameters were investigated, which are recorded in the production data sheet of each PC. Among the investigated parameters the most important were: pressure and temperature in the chamber before, during and after evaporation, residual gas composition with emphasis on the partial pressure of H_2O and hydrocarbons, status of the chamber (number of evaporations since last cleaning of chamber), outgassing (duration of pumping cycles), evaporation rate, CsI layer thickness, CsI powder history, source heating time until the

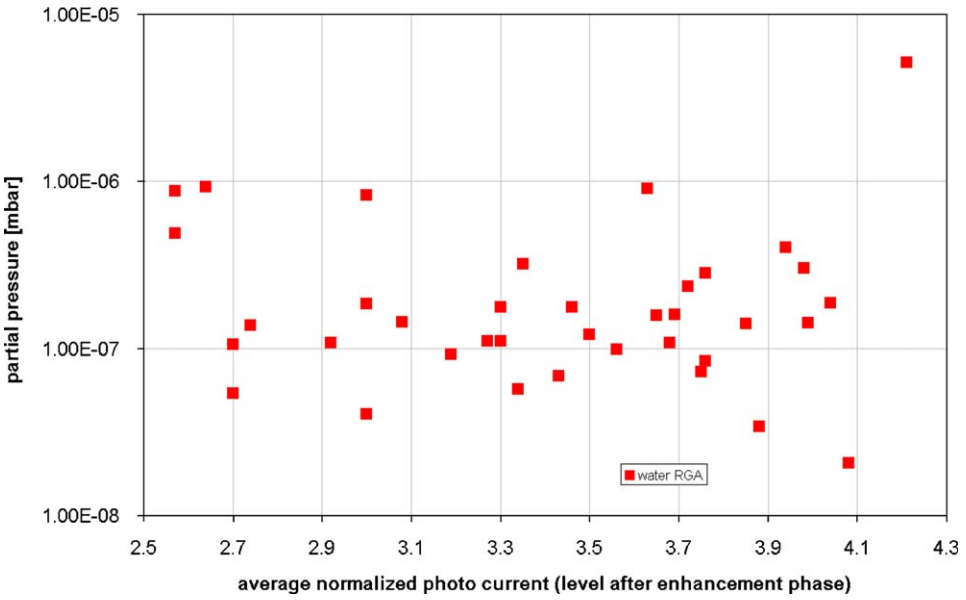

Fig. 9. Plot of the partial pressure of H_2O in the chamber before evaporation against the normalized photo-current on the PCs after the enhancement phase.

start of the evaporation, etc. The attempt to find a clear correlation between one of these parameters and either the final level of the photo-current or the rate of current increase during the enhancement phase proved to be futile. Fig. 9 is only one example which shows a plot of the average photo-current of the PC against the partial pressure of water in the chamber before evaporation. At present it is assumed that the enhancement effect is determined by more than one parameter which influences the presence, location and movements of H_2O inside the chamber (see discussion in Section 5). Due to the rather complicated geometrical situation inside the plant it could be significant, where exactly the partial pressure is measured. The observation of a different response of the penning gauge and the RGA system during a deposition process supports this hypothesis: the penning gauge located at the evaporation side of the chamber (Fig. 1) registers a change in pressure during evaporation, to which the RGA system seems to be oblivious, as it is located on the other side of the chamber, which is partly shielded from the evaporation by means of an aluminium wall.

4.3. Treatments for badly performing PCs

The examples for badly performing PCs in Figs. 7 and 8 show the development until a few hours after CsI deposition. Usually the photo-current from these PCs started to increase very slowly during the following days or even weeks. As will be discussed in Section 5, the enhancement effect is believed to be a combination of structural change in the CsI layer and removal of H_2O from the film, which is somehow inhibited and then starts later at a much slower rate for the badly performing PCs. It was attempted to find new treatments to accelerate or trigger the enhancement with promising results. However, as pointed out above, the total fraction of PCs with the unsuccessful enhancement type was 20%, i.e. less than 10 PCs for the whole production. Therefore only a limited number of tests could be carried out and the results could not be reproduced with satisfying statistics to draw definitive conclusions. The results mentioned in the following paragraph are therefore presented only to provide an incentive for further tests to achieve a perfection of the technology and to motivate the discussion below.

One attempt to treat the badly performing PCs was to continue the heating outside the vacuum chamber, from which the PCs had to be extracted in order to continue the production. Therefore several PCs were transferred to an external oven in which they were kept at 60 °C for a week while being continuously flushed with dry Ar. Later the PCs were transferred back to the VUV-scanner where they usually showed an increased quality (10–20%). At this point, however, no statements can be made about the optimum duration and temperature of such a treatment.

Another way to trigger the enhancement was motivated by the past experience with PCs exposed to air. A limited exposure to humid air causes a decrease in QE which can be recovered by heating the PC again under vacuum [14]. This behaviour was also reproduced in tests with the VUV-scanner [3]. In one test the current level on the PC was slightly higher after the exposure–recovery cycle than before. Therefore it was attempted to expose PCs, which exhibited a lack of enhancement. The test showed that after exposure and renewed heating the enhancement was much faster than before and higher current levels could be achieved than before. Fig. 10 shows the current levels at different stages of the treatment of a test PC (Au-coated glass substrate). This could support the theory of an

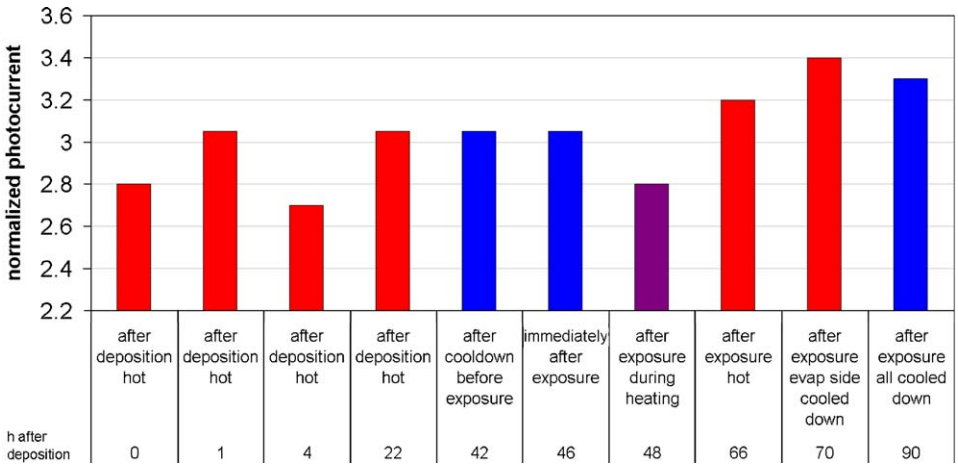

Fig. 10. Acceleration of the photo-current enhancement by means of exposure and re-heating of a test PC. The slowly enhancing PC was exposed to 250 mbar of air (room temperature, 40% relative humidity) during 1 h. Afterwards it was heated under vacuum and showed a faster enhancement. Current levels at different stages of the procedure are given.

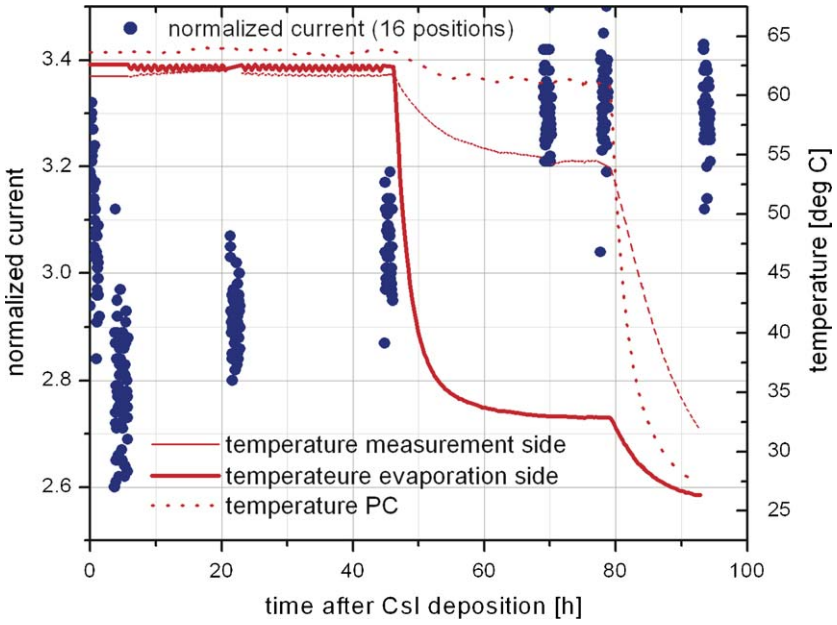

Fig. 11. Accelerated enhancement of PC 82 due to a cool-down of the evaporation side of the plant while the PC is still hot. The presence of cool, CsI coated surfaces is assumed to facilitate the removal of water from the PC.

enhancement consisting of a structural change in the CsI layer which is accelerated in the presence of H_2O. However also the subsequent removal of the water by heating seems to be part of the process. E.g. it was found that the current on the PC shows an increase, when the evaporation side of the chamber is cooled down first, while the PC on the scanner side is still at high temperature—compare Fig. 10. In this case the hygroscopic CsI layers present on the evaporation side act like a getter pump facilitating the removal of water from the hot PC—see Section 5.1. This behaviour could recently be reproduced in the final stages of the series production: Fig. 11 shows the development of a PC initially exhibiting the unsuccessful enhancement. During the following phase of slow enhancement the evaporation side of the chamber was cooled down first with the PC on the hot measurement side. The result was an accelerated enhancement. The high current level was found stable during the following cool-down of the whole chamber.

4.4. Summary of the investigation

The results of the investigation of the unsuccessful heat enhancement of some PCs can be summarized as follows:

- The substrates used in our evaporations are not directly responsible for the difference in behaviour: both types of behaviour can be reproduced with and without PCB in

the chamber; witness samples made from different substrates always behave like the large area PC.
- No clear correlation of the evaporation parameters such as pressure, residual gas composition or evaporation rate with the enhancement behaviour has been found. It is assumed that a combination of parameters influences the process through their influence on the quantity and exact location of water inside the chamber—see Section 5.
- External heating of PCs has a positive influence on badly performing PCs.
- A brief exposure of a badly performing PC to air and subsequent heating usually increases the enhancement rate.
- Cooling down the CsI coated chamber walls and the PC separately favours the enhancement process, presumably through increased water removal from the hot PC.

5. Discussion

The following paragraphs on vacuum, the relationship between CsI and water, and film growth summarize our current understanding of the processes involved in the CsI film deposition and heat enhancement as derived from the experience obtained during the series production and the tests performed beforehand. Even though the CsI deposition facility could not be primarily used as a research tool due to the needs of the production for the HMPID detector and consequently not all the observed effects could be studied systematically, the observations and results have contributed new insights into the production and treatment procedures and involved processes. In the following we are trying to put forward some ideas about the underlying processes in order to offer possible explanations for the observed effects and to provoke a discussion and further R&D, which is clearly necessary to improve—and even more importantly to control—the quality of CsI PCs for any future applications.

5.1. CsI and vacuum

In a vacuum system such as the CERN CsI deposition facility, which is not designed for ultra-high vacuum (UHV), the residual gas is always dominated by H_2O—compare Fig. 2. Water plays a special role in vacuum technology due to its adsorption properties on metal walls [20] and other surfaces. Other types of molecules do not influence the vacuum quality because they are either adsorbed strongly to the chamber walls and their desorption is negligible or because they do not stick at all or desorb at a very high rate and are readily removed by the pumping system. The behaviour of H_2O on the other hand is just in between the two extreme cases: its bonding capability to metal surfaces is high enough to cover all surfaces with multiple layers of water (with decreasing bonding strength from layer to layer) whenever the chamber is opened to air [20]. When the system is pumped, the water desorbs rather slowly and defines the pressure in the chamber. In the molecular flow regime, which is characterized by mean free paths that are longer than the extensions of the vacuum vessel, water molecules desorb from a surface, move on a straight line and stick to the next surface unless they reach the pump port. Thus the residual pressure in the chamber is defined by a dynamic equilibrium influenced by desorption, absorption and pumping, and dominated by water over a large timescale [20]. In the CERN CsI deposition chamber a pressure of $\geqslant 10^{-7}$ mbar is achieved with a water concentration of 80–90% (compare Fig. 2). At such a pressure the impingement rate of water is ≈ 0.1 monolayers (ML) per second on any surface. Therefore waterlayers can be supposed to be present in all processes. The most important means to increase water desorption is heating the vacuum vessel. Stainless steel UHV vessels are normally baked at 250–300 °C, but even the moderate temperature of 60 °C achieved in the CsI deposition chamber increases desorption, as can be seen from the pressure decrease of up to one order of magnitude during cool-down to room temperature after several days of pumping at 60 °C.

The presence of CsI in the chamber strongly affects the vacuum conditions and water migration due to the hygroscopicity of the material. CsI layers on the evaporation chamber walls act like a getter pump. Up to a certain extent water is trapped and desorption and water removal are slowed down further compared to other vacuum systems. In addition to these affects, dependencies of the conditions on the history of exposure to air during transfers and maintenance arise, i.e. if the CsI layers are exposed to air for a long time they will be saturated with water and introduce much more water to the chamber than usual. Consequently, the conditions in the chamber will depend on several parameters some of which are not easy to control: evaporation history (how many layers of CsI are present), maintenance history (how long was the chamber open), relative humidity of the air inside the lab during maintenance, heating cycles and temperature gradients. From what has been said about the movement of water from wall to wall and about thermally induced desorption, it is clear that the temperature differences inside the chamber will cause a transport of water from the hot to the cold surfaces. This has to be considered for the heat enhancement of CsI PCs, which might depend significantly on how the heating of the PC is performed, i.e. if only the PC is heated or the whole chamber—see test results in Section 4.3, Figs. 10 and 11.

5.2. CsI and H_2O

CsI is an alkali halide which forms ionic crystals quite similar to salt[5] (NaCl). Therefore CsI can easily be dissolved in water and is highly hygroscopic. Studies of

[5]The cubic crystalline structure is different from NaCl due to the larger size of the Cs-ion–CsCl type cubic.

water on NaCl crystals, which is a much better investigated system due to the importance of salt in everyday life, show that water forms layers on crystal surfaces. The work in Ref. [21] investigates the coverage of a NaCl crystal with water layers as a function of the humidity of the environment and shows the presence of a disordered water layer even under UHV conditions (10^{-9}) mbar and the influence of the water layer on the electronic states at the interface crystal–water. At higher humidities multiple layers are formed as discussed in Ref. [22]. If the coverage exceeds 2–3 ML the water starts to dissolve the crystal and the surface layers exhibit the properties of a saturated salt solution.

In the context of thin film CsI PCs limited exposure to humidity (humid air, humidified gases) is known to decrease QE [2,3,14]. Unless the exposure is long enough to completely destroy the film, the QE can be restored by heating the PCs. Heat enhanced PCs are thought to be more resistant to exposure (Ref. [14] and references therein). Investigations of CsI samples under the electron microscope have shown an increase of the grain size in the CsI film when exposed to humidity. In Ref. [2] an increase of the grain size up to the point where the film becomes discontinuous is shown. In Ref. [9] secondary electron microscope (SEM) pictures of a heat enhanced CsI film transferred under vacuum to the SEM show a grain size of approximately ≈ 100 nm before exposure and of up to 300 nm ($\approx$ film thickness!) after exposure to air in the lab. No further change in grain size has been observed when the sample was heated in the SEM after exposure, i.e. the grains remained large, although this treatment is known to restore the QE. The growth of CsI grains could be explained by a diffusion process which is accelerated by water. The presence of the polar H_2O molecule weakens the binding of the Cs and I ions in the crystal, i.e. lowers the activation energy E_A for diffusion and consequently diffusion rates increase as they are proportional to $\exp(-E_A/k_B T)$. Diffusion is also an important mechanism during the film deposition—see Section 5.3. Another property of CsI which changes due to exposure to humidity is volume resistivity [17], which decreases dramatically (several orders of magnitude) when the film is exposed to humid air. This could be connected both to the presence of water which increases mobility of ions in the film (see the above mentioned idea of a saturated ionic solution for high water coverages [22]) and to the change in grain size as the grain boundaries can trap charge carriers. However, the resistivity increases again when the vacuum is restored, whereas the grain size is not found or expected to change. Therefore the change in resistivity seems to be rather correlated with the adsorption and desorption of water on the film than with the change in grain size which happens in parallel. Furthermore, both the material in Ref. [17] and similar measurements in the CERN CsI deposition facility show the resistivity to increase during the heat enhancement phase, which suggests that also the enhancement effect is at least partly correlated with the removal of water.

Due to the impingement rate stated above (Section 5.1) water can be assumed to be present on the CsI film in vacuum and the same is true for storage or operation of the PC under dry gas at atmospheric pressure, if one considers that the usual contamination of a dry gas with water is in the part per million (ppm) range which corresponds to a partial pressure of 10^{-3} mbar/ppm and correspondingly high impingement rates.

Given these strong arguments for the presence of water layers on top of the CsI film, the question is how do they affect the QE. Apart from inducing a structural change, there are two ways in which the water can influence the QE: by absorbing the UV photons or by trapping the escaping photo-electrons. The absorption of UV photons by a few ML of water is very small and can only be relevant below 165 nm wavelength. According to data in Ref. [23] the transmittance of 1 nm liquid water is 99.8% for $\lambda = 165$ nm. The influence on the escaping photo-electrons on the other hand is much more relevant, especially in the long wavelength range close to the photoemission threshold. A photo-electron created by such a photon will have very little energy when it reaches the surface of the CsI film and it will be hydrated by the water molecules and effectively trapped, e.g. inside a cluster of water molecules[6] [24]. Coming back to the idea that the heat enhancement of CsI PCs is connected to the removal of water from the surface of the film, the trapping of low energetic photo-electrons explains very well why the heat enhancement is mainly effective in the long wavelength range and effectively lowers the photoemission threshold as mentioned in Section 3.1, as the likelihood for the low energetic photo-electron to be hydrated depends on the thickness of the water layer on top of the film.

5.3. Considerations on film growth

The (heat enhanced) CsI film exhibits a columnar structure as mentioned above (100 nm grain size of a 300–400 nm thick film). To answer the question how this structure arises and how it is influenced by the film deposition conditions, it can be very instructive to refer to the "structural zones" model for film growth which is described in many books on thin films, e.g. Ref. [27]. In the framework of this model the film structure is mainly defined by the rate of arriving molecules (adsorption rate) and by their diffusion capabilities on the surface of the film. Diffusion rates depend on the reduced temperature[7] T_S/T_M and therefore the film structure is predicted to change as a function of T_S/T_M. In the case of film deposition by evaporation under vacuum the model predicts three different types of structures.

[6] Due to their importance in chemistry such hydrated or solvated electrons are widely investigated, not only in the context of water or solutions [25] but also for the case of electron transport through a metal-oxide surface with adsorbed water at the interface [26].

[7] T_S is the substrate temperature, T_M the melting point of the film material.

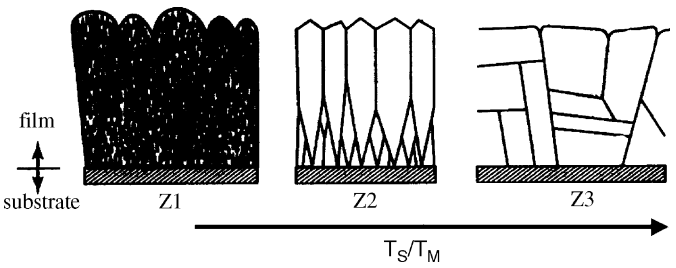

Fig. 12. Structural zones model: film structures for evaporation under vacuum.

The first structure (zone 1, Fig. 12) is realized for $T_S/T_M \leqslant 0.3$ when surface diffusion is negligible. The molecules cannot move far across the film before they are covered by the newly arriving ones which leads to a highly disordered porous columnar structure with small diameters (≈ 10 nm). In this case the surface roughness of the substrate has a high influence on the final structure (shadowing effects, voids). The second type of structure (zone 2, Fig. 12) arises for $0.5 \geqslant T_S/T_M \geqslant 0.3$ when surface diffusion becomes increasingly important and the arriving molecules have enough time to form larger islands which will grow into larger columns with facetted tops resulting in a denser film which is less dependent on the surface roughness of the substrate compared to zone 1. The third type of structure with $T_S/T_M \geqslant 0.5$ is formed if not only surface but also bulk diffusion becomes relevant during the growth process resulting in recrystallization during growth and Ostwald ripening.[8] This leads to larger equiaxed grains (grain size up to film thickness). The transition between the different structures can be quite sharp. According to the above mentioned morphological information about CsI films[9] the thin film PC structure is best described by zone 2, which stresses the fact that (surface) diffusion is an important process in the CsI film growth, as is also confirmed by surface diffusion constants given in Ref. [28]. It was already speculated in the previous section that the presence of water may increase diffusion and lead to the growth of larger grains. However, in the comparison with this model one should keep in mind that the diffusion processes might be quite different in the case of CsI due to the above mentioned possibility of ionic diffusion for high water coverages. Due to the high impingement rate of water during the coating process (≈ 0.1–1 ML/s) and the hygroscopicity of CsI a significant amount of water might be incorporated into the film which grows with a rate of $1\,\text{nm/s} \approx 2.2\,\text{ML/s}$. Therefore already at this stage the water conditions in the chamber determine the structure of the film due to their influence on diffusion inside/on the film, supplementing or maybe even outweighing the influence of T_S/T_M. The third structure including the process of grain growth seems to describe the behaviour of the CsI layer when exposed to humid air as described above, indicating that the hydration even leads to bulk diffusion.

Apart from the above discussed role of water, differences in morphology or grain size themselves are likely to influence the QE. The form of the grain tops define the surface which is available for photo-electron extraction, i.e. a very rough surface of the CsI layer surface should increase the QE as pointed out in Ref. [29]. On the other hand smaller grains can also have a detrimental effect due to the increased number of grain boundary interfaces which are likely to trap photo-electrons and prevent them from leaving the film. As already stated above in Section 4.3, the enhancement of the QE following the film deposition might not only be related to the removal of water from the layer surface, but also to a structural change in the film promoted by the diffusion processes which in turn are influenced by the water content and coverage of the layer. The structural change might be a settling of the film into a certain grain structure, e.g. by filling out voids and grain growth or even a re-crystallization, maybe a transition starting from a zone 1 type structure. Such a structural change involving the filling of voids and thus leading to a denser layer with larger grains would also explain the improved resistance of the heat enhanced CsI to exposure to humidity, as a non-enhanced, more porous film is much easily attacked by adsorbed water than a dense structure. The most likely explanation is a combination of the two mentioned processes: a structural change followed by the removal of water at first from the bulk and then from the surface. Within these hypotheses about the possible roles of water several experimental observations can be tentatively explained:

- A unsuccessful enhancement or slow enhancement of a PC could have two reasons: either an inefficiency to perform the structural change (lack of water inside the film and low temperature) or an inefficiency to finally remove the water from the surface (bad vacuum, saturated CsI on the walls of the evaporation chamber).
- The drop of the photo-current, which is observed in the unsuccessful enhancement type shown in Fig. 7(b), could be interpreted as an intermediate stage during which water is transported from the bulk of the CsI to the surface. Thus any diffusion driven structural change would be interrupted, and the presence of water at the surface would lower the escape probability of low energetic photo-electrons. A subsequent slow desorption of the water from the surface explains the following slow increase of the PC response. However, in an alternative explanation the drop could be attributed to a transport of water to the PC from parts of the chamber with a temperature higher than that at the PC surface.
- The observation of an enhancement provoked by briefly exposing the PC to air, as described in Section 4.3 and Fig. 10, can be explained as follows: at first the film is not able to undergo the structural change but this

[8] Larger grains start growing while small grains disappear.

[9] The deposition of CsI ($T_M = 626\,^\circ\text{C} = 899\,\text{K}$) at $T_S = 60\,^\circ\text{C} = 333\,\text{K}$ corresponds to a $T_S/T_M = 0.37$.

changes, when it is exposed and the adsorbing water provides the necessary mobility. Later, when the film is heated again, the water leaves the film and desorbs resulting in the faster QE increase.

5.4. Other factors contributing to the PC QE and its evolution in time

Of course the role of water, which was discussed in the previous sections, is not the only factor affecting the CsI quantum efficiency and its evolution. Besides water there are other molecules present in the residual gas and especially on surfaces in the form of a coverage of one or several ML. Thus during the evaporation not only CsI molecules hit the photocathode substrate but other molecules as well. To top it all the evaporated CsI does not form ideal crystalline structure. It contains a number of various defects: cracks, vacancies, insertions, dislocations and so on as well as chemical impurities. Lattice defects change the electronic levels in the vicinity of defects and create additional electronic levels within the band-gap. This in turn will change the light absorption characteristics and also may create traps for holes and electrons (so called V and F centres) and all these together will affect the shape of the quantum efficiency curves as well as the absolute value of the QE (see for example Ref. [30]). It is known that heat treatment changes the population and dynamics of the additional levels and thus causes changes in QE. Experiments performed by various authors as well as our data suggest, however, that the main contribution to the heat enhancement effect results from water contamination. Indeed, the first heat enhancement effect observed in Ref. [31] was obtained when only the photocathode was heated and the rest of the chamber was kept at room temperature. In this case the water evaporated from the photocathode was absorbed at the cold chamber walls which allowed a very efficient water removal from the photocathode. When both chamber and PC were heated, no strong enhancement was observed. In some cases this even caused a degradation of the QE, probably due to the water evaporating from the walls of the chamber. These results are in agreement with the observation of an increase in QE in a cool-down of only half of the set-up while the PC is kept hot, which has been described above (Section 4.3). This is a good indication that the most important procedure is not only the heating of the photocathode (as a way of annealing possible defects and extra levels), but creating conditions in which the water molecules liberated from the photocathode can migrate to cooled walls or to a powerful pumping system, e.g. including a getter pump or cold trap.

5.5. Further R&D required

For possible future applications of CsI PCs an increased understanding of the discussed effects is preferable in order to achieve a better control of the production process, lower the quality spread of photocathodes and maximize the QE. Therefore additional R&D efforts should be made to investigate the behaviour of the CsI PCs with an emphasis on the best possible control of water, i.e. starting by testing small samples in a UHV chamber to remove the influence of water as far as possible and then comparing with the situation in an environment more similar to a large area production facility, i.e. with higher residual pressures. Such a system should provide the possibility to do an in situ investigation of the photo-current, morphology and also conductivity.[10] It should as well be attempted to investigate if the observed effects are accompanied by structural changes, i.e. surface sensitive diffraction analysis, e.g. Low Energy Electron Diffraction (LEED) or grazing incidence X-ray diffraction. If an in situ investigation is not feasible the transport of the samples has to be carried out under vacuum, as even a transport under dry gas increases the partial pressure of water contaminations by several orders of magnitude. The aim should be to investigate changes in the CsI layer immediately after film deposition (rather small time window!) correlated with heating, which would require the capability of heating the samples during the various tests. The heating method itself should be investigated, especially the difference between heating only the samples or heating the whole system as mentioned above. Another important quantity to be included in the investigation is film density. Both the water content of the film and the morphological structure of the film discussed in the previous section will result in different densities, which should consequently be monitored.[11] The knowledge of the film density would also constitute an important input parameter for a possible simulation of the film growth.

5.6. Conclusions for the HMPID detector

Despite the requirement to perform additional tests to fully understand all the underlying effects, the established procedure allows to produce high quality CsI PCs. Such CsI PCs are currently used or have been used successfully in RICH layouts in several experiments [32–35]. Due to this experience and the results on long term stability and ageing obtained in the past [36,37] as well as from ongoing tests with the ALICE/HMPID PCs, the recently completed HMPID modules are expected to perform particle identification as required in or even exceeding the design specifications for the detector. A QE curve for each PC obtained from beam tests and from ongoing tests with cosmic rays, combined with the surface mapping of the photo-current for each of the 42 PCs, provides QE data for the physics analysis in unprecedented resolution. The series production of CsI PCs for the detector has accumulated valuable insights into the technology of large area thin film

[10] E.g. simultaneous coating and treatment of micro-strips [17] and samples.

[11] E.g. by inspecting a broken piece of the layer under the SEM at different stages.

CsI PCs, e.g. by establishing the importance of post deposition enhancement and of the complex interactions of the PCs with residual water present at all stages from deposition to storage and operation.

Acknowledgements

The operation of the VUV-scanner and the production of the PCs rely on the competent support provided by the technical staff at CERN. We would like to thank M. van Stenis, X. Pons, J.B. van Beelen, P. Ijzermans, C. David, M. Malabaila, B. Cantin and D. Fraissard.

References

[1] ALICE Collaboration, J. Phys. G 30 (2004) 1517.
[2] ALICE Collaboration, ALICE HMPID Technical Design Report, CERN/LHCC 98/19.
[3] H. Hoedlmoser, et al., Nucl. Instr. and Meth. A. 2006, in press, doi: 10.1016/j.nima.2006.07.052.
[4] E. Schyns, Nucl. Instr. and Meth. A 494 (2002) 441.
[5] A. Braem, et al., Nucl. Instr. and Meth. A 502 (2003) 205.
[6] A. Gallas, et al., Nucl. Instr. and Meth. A 553 (2005) 345.
[7] A. Di Mauro, et al., Nucl. Instr. and Meth. A 433 (1999) 190.
[8] H. Hoedlmoser, et al., Nucl. Instr. and Meth. A 553 (2005) 140.
[9] H. Hoedlmoser, CERN-THESIS-2006-004.
[10] D.F. Anderson, S. Kwan, V. Peskow, B. Hoeneisen, Nucl. Instr. and Meth. A 323 (1992) 626.
[11] H. Brauning, et al., Nucl. Instr. and Meth. A 327 (1993) 369.
[14] Breskin, Nucl. Instr. and Meth. A 371 (1996) 116.
[17] J. Va'vra, et al., Nucl. Instr. and Meth. A 387 (1997) 154.
[20] A. Berman, Vacuum 47 (4) (1996) 327.
[21] J. Arsic, et al., J. Chem. Phys. 120 (20) (2004) 9720.
[22] S.J. Peters, G.E. Ewing, Langmuir 13 (24) (1997) 6345.
[23] Hayashi, et al., Proc. Natl. Acad. Sci. 97 (12) (2000) 6264.
[24] K.S. Kim, et al., Phys. Rev. Lett. 76 (6) (1996) 956.
[25] C.M.R. Clancy, M.D.E. Forbes, Inter-American Photochemical Society Newsletter, vol. 22(1), 1999, p. 16.
[26] K. Onda, et al., Science 308 (2005) 1154.
[27] M. Ohring, The Materials Science of Thin Films, Academic Press, New York, 1992.
[28] M.H. Yang, C.P. Flynn, Phys. Rev. Lett. 62 (21) (1989) 2477.
[29] M.A. Nitti, et al., Nucl. Instr. and Meth. A 553 (2005) 157.
[30] A.J. Dekker, Solid State Physics, MacMillan, London, 1958.
[31] D.F. Anderson, et al., Results on CsI enhancement and aging Fermilab technical meme TM-175, 1991.
[32] K. Zeitelhack, et al., Nucl. Instr. and Meth. A 433 (1999) 201 (and references therein).
[33] G. Baum, et al., Nucl. Instr. and Meth. A 433 (1999) 201 (and references therein).
[34] F. Garibaldi, et al., Nucl. Instr. and Meth. A 502 (2003) 117 (and references therein).
[35] I. Tserruya, Nucl. Instr. and Meth. A 553 (2005) 196.
[36] A. Braem, et al., Nucl. Instr. and Meth. A 553 (2005) 187.
[37] A. Braem, et al., Nucl. Instr. and Meth. A 515 (2003) 307.